Impaired Tethering and Fusion of GLUT4 Vesicles in Insulin-Resistant Human Adipose Cells

Vladimir A. Lizunov,[1] Jo-Ping Lee,[2] Monica C. Skarulis,[3] Joshua Zimmerberg,[1] Samuel W. Cushman,[2] and Karin G. Stenkula[2,4]

Systemic glucose homeostasis is profoundly influenced by adipose cell function. Here we investigated GLUT4 dynamics in living adipose cells from human subjects with varying BMI and insulin sensitivity index (S_i) values. Cells were transfected with hemagglutinin (HA)-GLUT4-green fluorescent protein (GFP)/mCherry (red fluorescence), and were imaged live using total internal reflection fluorescence and confocal microscopy. HA-GLUT4-GFP redistribution to the plasma membrane (PM) was quantified by surface-exposed HA epitope. In the basal state, GLUT4 storage vesicle (GSV) trafficking to and fusion with the PM were invariant with donor subject S_i, as was total cell-surface GLUT4. In cells from insulin-sensitive subjects, insulin augmented GSV tethering and fusion approximately threefold, resulting in a corresponding increase in total PM GLUT4. However, with decreasing S_i, these effects diminished progressively. All insulin-induced effects on GLUT4 redistribution and trafficking correlated strongly with S_i and only weakly with BMI. Thus, while basal GLUT4 dynamics and total cell-surface GLUT4 are intact in human adipose cells, independent of donor S_i, cells from insulin-resistant donors show markedly impaired GSV tethering and fusion responses to insulin, even after overnight culture. This altered insulin responsiveness is consistent with the hypothesis that adipose cellular dysfunction is a primary contributor to systemic metabolic dysfunction. ***Diabetes*** **62:3114–3119, 2013**

The development of insulin resistance is strongly linked to obesity. Despite this association, not all obese individuals carry metabolic and cardiovascular risk (1,2). It is well recognized that relatively lean individuals can exhibit insulin resistance and conversely, obese individuals can be insulin sensitive (3,4). Adipose tissue plays a crucial regulatory function that integrates lipid and glucose metabolism, and exerts significant influence over the metabolic function of other tissues via adipokines (5,6). Another important regulatory function of adipose tissue comprises the control of stored fat distribution among fat depots, muscle, and liver where increased ectopic fat storage is highly associated with systemic insulin resistance (7).

From the [1]Program in Physical Biology, Eunice Kennedy Shriver National Institute of Child Health and Human Development, National Institutes of Health, Bethesda, Maryland; the [2]Experimental Diabetes, Metabolism, and Nutrition Section, National Institutes of Health, Bethesda, Maryland; the [3]Diabetes, Endocrinology, and Obesity Branch, National Institute of Diabetes and Digestive and Kidney Diseases, National Institutes of Health, Bethesda, Maryland; and [4]Experimental Medical Sciences, Lund University, Lund, Sweden.
Corresponding author: Joshua Zimmerberg, joshz@mail.nih.gov.
Received 12 December 2012 and accepted 20 May 2013.
DOI: 10.2337/db12-1741
This article contains Supplementary Data online at http://diabetes.diabetesjournals.org/lookup/suppl/doi:10.2337/db12-1741/-/DC1.
J.-P.L. is currently affiliated with the Industrial Technology Research Institute, Chutung, Hsinchu, Taiwan, Republic of China.

Facilitative GLUT4 is the key molecule responsible for insulin-stimulated glucose uptake, and its ability to function is determined by translocation of intracellular GLUT4 storage vesicles (GSVs) (8), tethering of GSVs to the plasma membrane (PM) (9), and GSV fusion with the PM, which finally delivers GLUT4 to the cell surface (10). Previous reports have demonstrated that adipose cells from insulin-resistant human subjects exhibit decreased expression of GLUT4 and impaired insulin signaling (11–13). Importantly, it was shown that selective downregulation of GLUT4 in adipose tissue inhibits the insulin response in muscle and induces systemic insulin resistance (7,14). Still, very few studies have focused on the GLUT4 translocation process in human adipose cells (15–17). Here, we examined the regulation of GLUT4 dynamics in adipose cells isolated from human subjects with a spectrum of systemic insulin resistance. We applied total internal reflection fluorescence (TIRF) microscopy to quantify the subcellular trafficking of GLUT4 and its regulation by insulin. We directly correlated systemic insulin sensitivity with insulin-dependent GLUT4 trafficking in adipose cells from subjects with widely varying degrees of insulin resistance and observed that the development of systemic insulin resistance is associated with cellular defects in insulin-stimulated GLUT4 translocation.

RESEARCH DESIGN AND METHODS

Subjects. Subjects consented to enroll in a National Institute of Diabetes and Digestive and Kidney Diseases institutional review board-approved study (Clinical trial reg. no. NCT00428987, clinicaltrials.gov) to extensively phenotype subjects with varying degrees of obesity. Patients with treated diabetes or advanced cardiovascular, kidney, or liver disease were excluded. Participants were admitted to the Metabolic Clinical Research Unit in the Hatfield Clinical Research Center at the National Institutes of Health after screening and demonstration of stable weight (within 3%) for at least 30 days prior to testing. Abdominal subcutaneous adipose tissue was biopsied by aspiration using a 16-gauge needle under local anesthesia (1% lidocaine). Intravenous glucose tolerance testing was performed in the morning after a 12-h overnight fast with two intravenous catheters placed in each antecubital vein according to the modified method of Bergman and colleagues (18). Insulin sensitivity index (S_i) was calculated from glucose and insulin measurements using the MinMod Millennium (6.02) (18). Body fat percentage was determined by dual-energy X-ray absorptiometry using a total body scanner (Lunar iDXA; GE Healthcare, Madison, WI).

Reagents. Insulin-responsive aminopeptidase (IRAP)-pHluorin (a pH-sensitive probe for fusion detection) was provided by T. Xu, and the IRAP-green fluorescent protein (GFP), by J.E. Pessin. Construction of hemagglutinin (HA)-GLUT4-mCherry (red fluorescence) has been described previously (19). Mouse monoclonal anti-HA-antibody (HA.11) was from Berkeley Antibody Company (Richmond, CA), and rabbit polyclonal anti-GLUT4-antiserum was generated by F. Hoffmann-La Roche Ltd. (Nutley, NJ), peptide affinity-purified (20) BSA (fraction V) was from Intergen (Purchase, NY), and collagenase was from Worthington (Lakewood, NJ). Dulbecco's modified Eagle's medium, insulin, and Alexa Fluor-conjugated antibodies were from Life Technologies (Grand Island, NY). Insulin was prepared as a stock (250 IU/mL) and diluted into Krebs-Ringer bicarbonate HEPES buffer, 1% BSA, to a final working concentration of 0.02 IU/mL.

Adipose cell isolation and transfection. Adipose cells were prepared as previously described (21). Transfection was by electroporation as previously

described (22), using a square-wave pulse (400 ms, 12 ms, one pulse), at a plasmid concentration of 4 μg/mL. Cells were kept in culture overnight in 15-mL plastic conical tubes at 37°C, 5% CO_2 in Dulbecco's modified Eagle's medium containing 25 mmol/L glucose, 50 IU/mL penicillin, 50 μg/mL streptomycin, 200 nmol/L (−)-N_6-(2-phenylisopropyl)adenosine, and 3.5% (weight for volume) BSA (22).

Microscopy and image analysis. For immunofluorescence microscopy, cells were stimulated with insulin for 30 min, fixed with 4% paraformaldehyde for 10 min, and labeled with anti-HA antibody (1:500) and secondary Alexa Fluor-647 antibody (1:500). Cells were imaged using a confocal microscope (LSM510; Zeiss) with a 63× 1.4 numerical aperture oil-immersion objective lens (23). For live-cell imaging, adipose cells were kept in Krebs-Ringer bicarbonate HEPES buffer (1% BSA, pH 7.4), maintained at 37°C using a temperature-controlled chamber (Δ-T; Bioptechs). Cells were imaged using an objective-based TIRF setup built around a Nikon TI microscope and coupled with a custom-built laser combiner system equipped with 405/488/561/640 nm lasers (Coherent) (24). A set of automated image processing ImageJ macro/subroutines was used for the analysis of individual vesicle trafficking and fusion, as described previously (19,23). Traffic intensity was estimated as the number of mobile vesicles (with trajectory length >2 μm) detected within a region of interest of 10 × 10 μm during 1 min. Trajectory maps were built from stacks of 60 images, representing 1 min of recording using the ImageJ projection plugin, to create "maximum intensity projection" and "mean intensity projection" images (18). Maximum intensity projection creates an output image each of whose pixels contains the maximum value over all images in the stack at the particular pixel location. Mean intensity projection outputs an image wherein each pixel stores the average intensity over all images in the stack at the corresponding pixel location. Then a resulting image is created wherein each pixel is assigned a value of the difference between corresponding maximum and mean intensity projection corresponding pixel values. The resulting image contains the traces of individual vesicles that were moving during the time of the recording.

Statistical analysis. All data are represented as means ± SEM, unless otherwise stated. Statistical significance was analyzed using Student t test or ANOVA. Simple and multiple regressions were carried out using the linear model function in R, version 2.10 (http://www.r-project.org).

RESULTS

Transfection of isolated human adipose cells. In order to evaluate the relationship between systemic glucose homeostasis and the translocation and cell-surface distribution of GLUT4 in human subjects, we isolated adipose cells from subcutaneous adipose tissue from subjects varying widely in BMI (24–62 kg/m^2) and S_i (0.2–11 min^{-1} per μU/mL) (Supplementary Tables 1 and 2). Isolated cells were transfected with HA-GLUT4-GFP or HA-GLUT4-mCherry plasmid, and exogenous protein was expressed during an overnight incubation. GLUT4 localization and subcellular trafficking were detected by conventional TIRF microscopy, with an expanded penetration depth (150–200 nm) that covered most of the microtubule-based intracellular traffic (Fig. 1*A* and Supplementary Video 1). IRAP, another known GSV resident, was coexpressed with GLUT4-mCherry to confirm the presence of GLUT4 in GSV. Consistent with previous studies of primary rat adipose cells (19), GSVs were scattered uniformly across the entire cytoplasm, and were labeled with both GLUT4-mCherry and IRAP-GFP (Fig. 1*B*). Translocation of GLUT4 to the PM was independently verified by confocal immunofluorescence microscopy using HA antibody to detect HA-GLUT4-GFP exposed on the cell surface (Fig. 1*C*).

Insulin-stimulated GLUT4 trafficking. From time-lapse TIRF microscopy recordings in adipose cells expressing HA-GLUT4-GFP, we obtained the number of mobile GSVs per unit of cell-surface area, which is illustrated in Fig. 2*A*. In the basal state, we recorded the traffic of mobile GSVs that resembles long-range movement associated with the microtubular network (9). The addition of insulin induced an increased tethering, reflected after 30 min of insulin

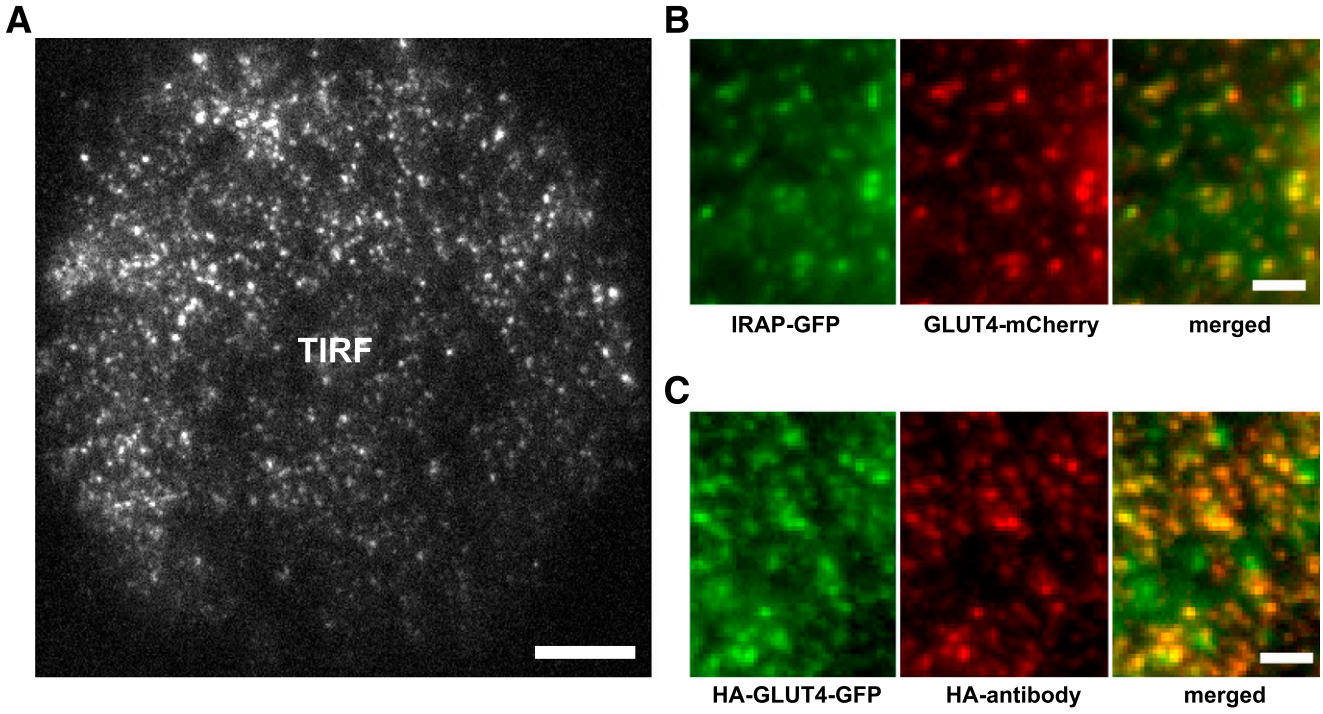

FIG. 1. Transfection of isolated human adipose cells: intracellular localization and exofacial detection of epitope-tagged GLUT4. *A*: High-resolution TIRF microscopy was used to detect HA-GLUT4-GFP in the thin layer of cytosol adjacent to the adipose cell PM. Scale bar is 10 μm. *B*: Magnified regions from adipose cells transfected with HA-GLUT4-mCherry and IRAP-GFP were imaged using TIRF microscopy and showed high colocalization of GLUT4 and IRAP, an independent marker of GSV. Scale bars are 2 μm. *C*: Translocation of HA-GLUT4-GFP to the PM was verified by TIRF microscopy detection of HA antibody binding to the extracellular loop of HA-GLUT4-GFP. Cells were stimulated with insulin for 30 min, fixed, stained with mouse-anti-HA antibody, and visualized using secondary goat-anti-mouse-Alexa Fluor 594 antibody. Scale bars are 2 μm.

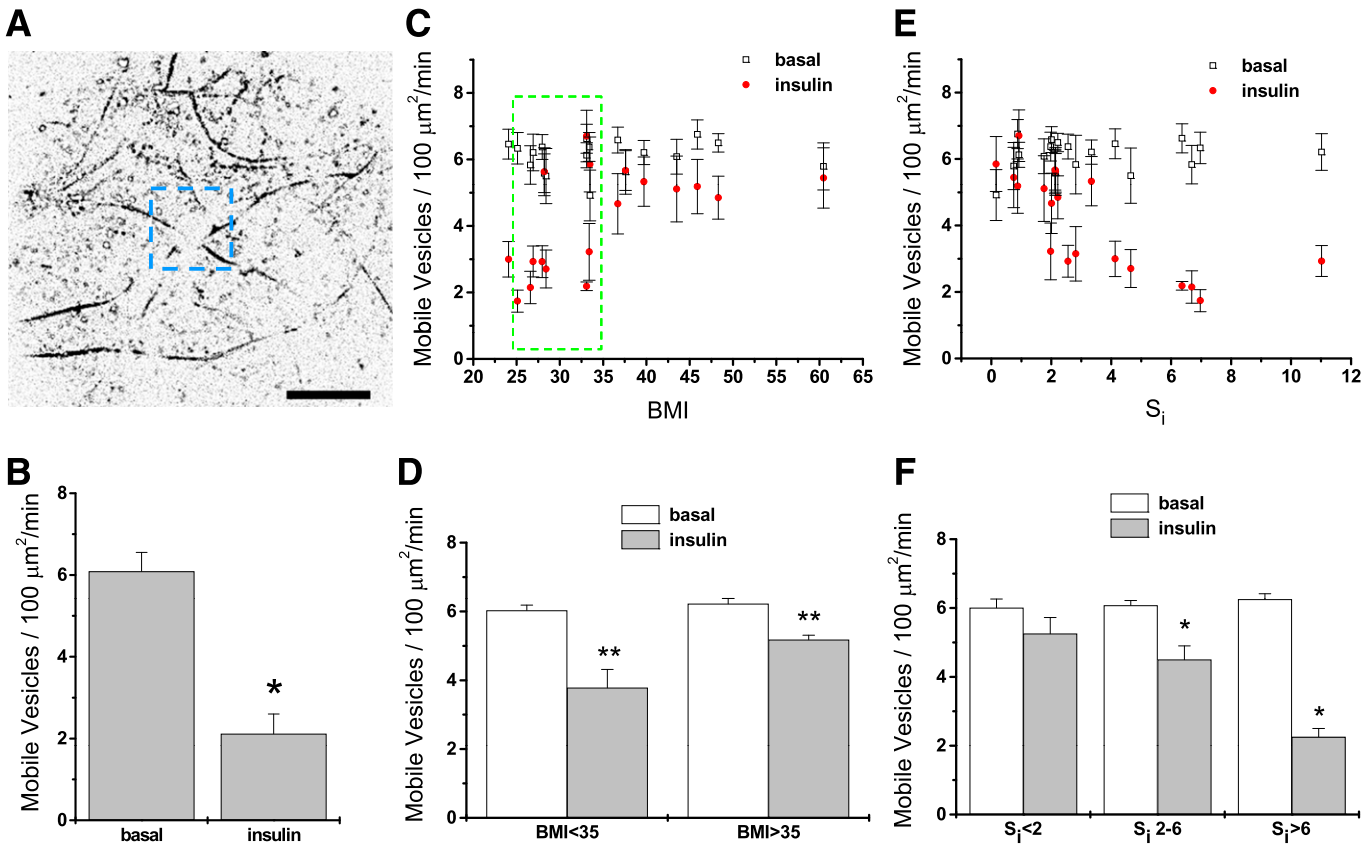

FIG. 2. Insulin-stimulated decrease of GSV trafficking. Isolated human adipose cells were transfected with HA-GLUT4-GFP, and GSV traffic was monitored using time-lapse TIRF microscopy in the basal and insulin-stimulated states. *A*: Trajectory maps were built from stacks of time-lapse images to obtain the traces of all GLUT4 vesicles moving in the vicinity of the PM. GLUT4 traffic intensity was estimated as the average number of mobile vesicles (with trajectory length >2 μm) detected within three to four regions of interest of 10 × 10 μm during 1 min of recording. Scale bars are 10 μm. *B*: Characteristic insulin-stimulated decrease of the number of mobile GSVs measured in adipose cells isolated from an insulin-sensitive subject. Mean ± SEM; $N = 9$. *$P < 0.05$. *C*: Number of the mobile GSVs detected in basal and insulin-stimulated cells plotted against the BMIs of the subjects. Cells from subjects with a BMI within the narrow range of 25–35 (dashed box) that displayed highly variable insulin responses were further analyzed for the effects of S_i independent of BMI (Supplementary Fig. 1). Mean ± SEM; $N = 9$. *D*: Number of mobile GSVs averaged across the subjects with a BMI <35 ($n = 10$) and BMI >35 ($n = 7$). Mean ± SEM; **$P < 0.01$. *E*: Number of the mobile GSVs plotted against the S_i of the subjects. *F*: Number of mobile GSVs averaged across three groups of subjects with different insulin sensitivity: low insulin sensitivity (S_i <2, $n = 6$), intermediate insulin sensitivity (S_i 2–6, $n = 9$), and normal insulin sensitivity (S_i >6, $n = 4$). All data are shown as means ± SEM. *$P < 0.05$.

stimulation in a significantly diminished number of mobile GSVs (Fig. 2*B*).

We further looked for alterations in the intracellular distribution and trafficking of GSVs associated with obesity (increased BMI) and/or systemic insulin resistance (decreased S_i). In the basal state, we found no significant differences in GSV dynamics among cells from subjects with varying values of either BMI or S_i (Fig. 2*C*–*F*). However, in response to insulin, cells from subjects with increasing BMI (Fig. 2*C* and *D*) or decreasing S_i (Fig. 2*E* and *F*) exhibited decreasing effects of insulin.

By dividing the human subjects into groups based on insulin sensitivity—low ($S_i < 2$), intermediate (S_i 2–6), and normal ($S_i > 6$) (Fig. 2*F*)—adipose cells from subjects with S_i 2–6 and $S_i > 6$ showed a significant decrease of GSV trafficking in response to insulin. Specifically, cells obtained from the most insulin-resistant subjects ($S_i < 2$) did not respond to insulin, while cells from the most insulin-sensitive subjects ($S_i > 6$) displayed the most pronounced insulin-induced effect on GSV dynamics.

Subjects with BMI values of 25–35 (Fig. 2*C*, outline, Supplementary Fig. 1*A* and *B*) had a broad range of systemic insulin sensitivity. Cells from these subjects displayed corresponding insulin responsiveness with a strong correlation to the subjects' S_i, but no significant correlation to BMI. Multiple linear regression of insulin-stimulated tethering against BMI and S_i together did not improve the correlation over that to S_i alone for this smaller group of subjects (Supplementary Fig. 1).

Insulin-stimulated GSV fusion with the PM. To examine the effect of insulin on GSV fusion, we investigated GSV exocytosis in human adipose cells cotransfected with HA-GLUT4-mCherry and IRAP-pHluorin using multicolor TIRF microscopy (23). As previously determined in rat adipose cells, the insulin-induced decrease in GSV trafficking is due to increased GSV tethering to the PM preceding fusion. Thus, we tested whether the impaired tethering of GSV seen in response to insulin in adipose cells of insulin-resistant or obese subjects led to a decrease in insulin-stimulated fusion. Figure 3*A*–*D* shows that the frequency of fusion events in the basal state does not vary with either BMI or S_i, but that the number of fusion events in response to insulin decreases with increasing BMI (Fig. 3*A* and *B*) or decreasing S_i (Fig. 3*C* and *D*). Cells analyzed from less obese subjects (BMI < 35) showed a threefold increase of fusion events in response to insulin compared with cells from more obese subjects (BMI > 35) that displayed a less than twofold increase (Fig. 3*B*). Further, adipose cells from

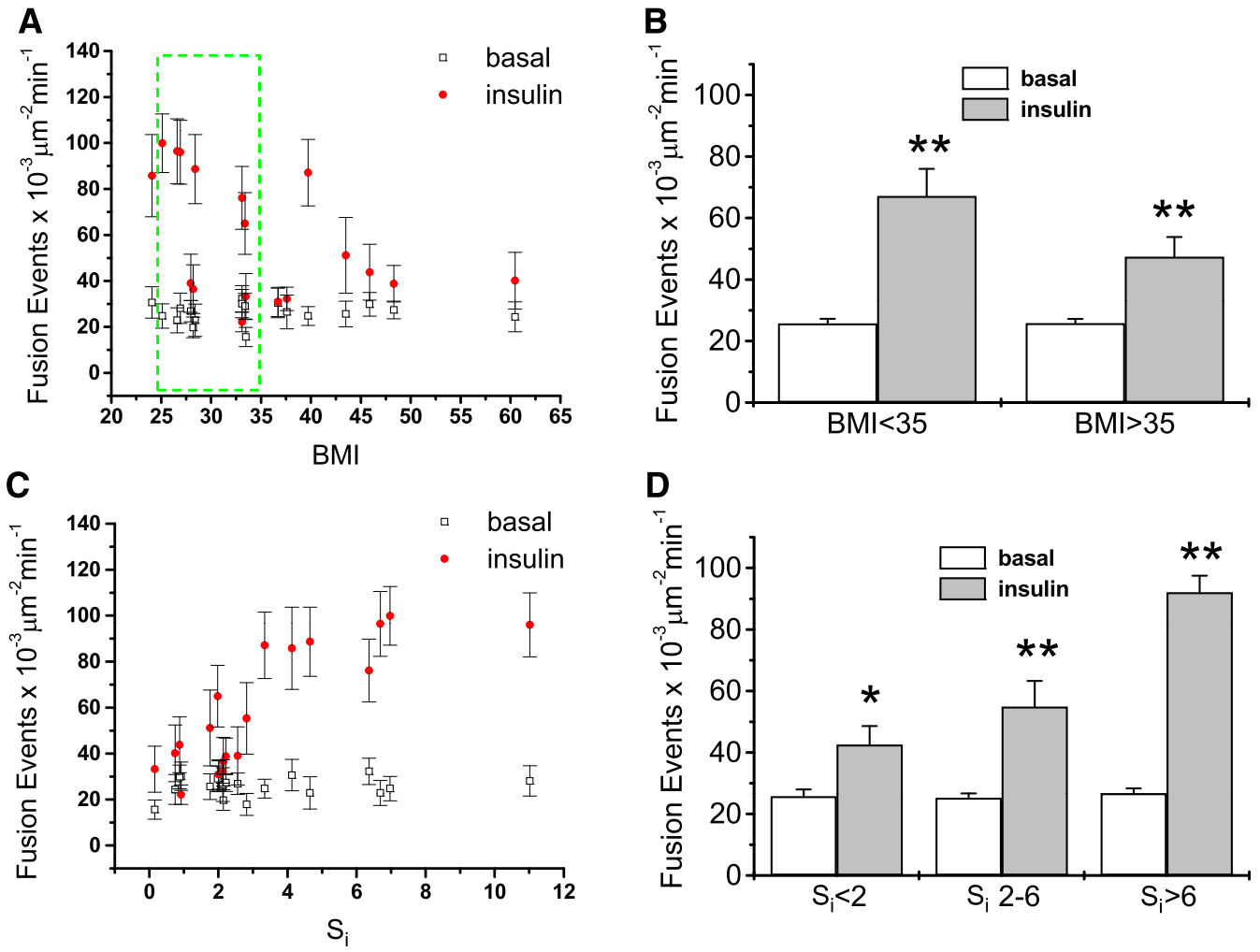

FIG. 3. Correlation of insulin-stimulated GSV fusion with BMI and S_i. GSV fusion events at the PM were measured by TIRF microscopy using IRAP-pHluorin. *A*: Frequency of fusion events plotted against BMI. Mean ± SEM; $N = 9$. Cells from subjects with BMI within the narrow range of 25–35 (dashed box) that displayed highly variable insulin responses were further analyzed for the effects of S_i independent of BMI (Supplementary Fig. 2). *B*: Frequency of fusion events averaged across the subjects with BMI <35 ($n = 10$) and BMI >35 ($n = 7$). Mean ± SEM; $^{**}P < 0.01$. *C*: Frequency of fusion events plotted against S_i. Mean ± SEM; $N = 9$. *D*: Frequency of fusion events averaged across three groups of subjects with different insulin sensitivity: low insulin sensitivity (S_i <2, $n = 6$), intermediate insulin sensitivity (S_i 2–6, $n = 9$), and normal insulin sensitivity (S_i >6, $n = 4$). Mean ± SEM; $^{*}P < 0.5$; $^{**}P < 0.01$.

the most insulin sensitive patients ($S_i > 6$) showed the greatest insulin response (Fig. 3*D*), in line with the data on GSV trafficking. Thus, we conclude that the impaired tethering in adipose cells of insulin-resistant subjects is followed by a decreased fusion frequency.

Again, among subjects with BMIs 25–35 (Fig. 3*A*, outline, Supplementary Fig. 2*A* and *B*), multiple linear regression of GSV fusion in the presence of insulin supports the concept that insulin responsiveness of adipose cells is in good correspondence with systemic S_i, but has only a weak dependence on either BMI.

Insulin sensitivity and GLUT4 distribution on the cell surface. To correlate PM GLUT4 with whole-body S_i, we measured cell-surface GLUT4 using an HA antibody-binding assay in transfected, isolated, nonpermeabilized cells (Fig. 4). In the basal state, we again found no significant differences in total cell-surface GLUT4 among cells from subjects with varying values of either BMI or S_i (Fig. 4*A* and *B*). However, insulin-stimulated total cell-surface GLUT4 decreased significantly with increasing BMI and decreasing S_i (Fig. 4*A* and *B*). Among subjects with BMIs 25–35 (Fig. 4*A*, outline, Supplementary Fig. 3*A* and *B*), insulin-stimulated total cell-surface GLUT4 correlated with systemic S_i, but did not show statistically significant correlations with BMI. Adipose cells isolated from subjects with $S_i > 6$ (the most insulin-responsive subjects) had the highest levels of GLUT4 present at the cell surface in the insulin-stimulated state (Fig. 4*C*).

DISCUSSION

In this study, we provide the first evidence of specific changes in GLUT4 translocation in isolated human adipose cells that reflect the systemic insulin sensitivity of the donor subjects. We show a direct impairment of insulin-stimulated GLUT4 translocation in cells from insulin-resistant subjects that is evident even after overnight culture, causing impaired GSV tethering that prevents them from entering the fusion process. Concomitantly, the amount of GLUT4 at the PM of insulin-stimulated cells was significantly decreased in insulin-resistant, compared with insulin-sensitive, subjects. Still, the machinery required for complete GLUT4 translocation was found intact since, in the basal state, the mobility of GSV on microtubules, the number of mobile

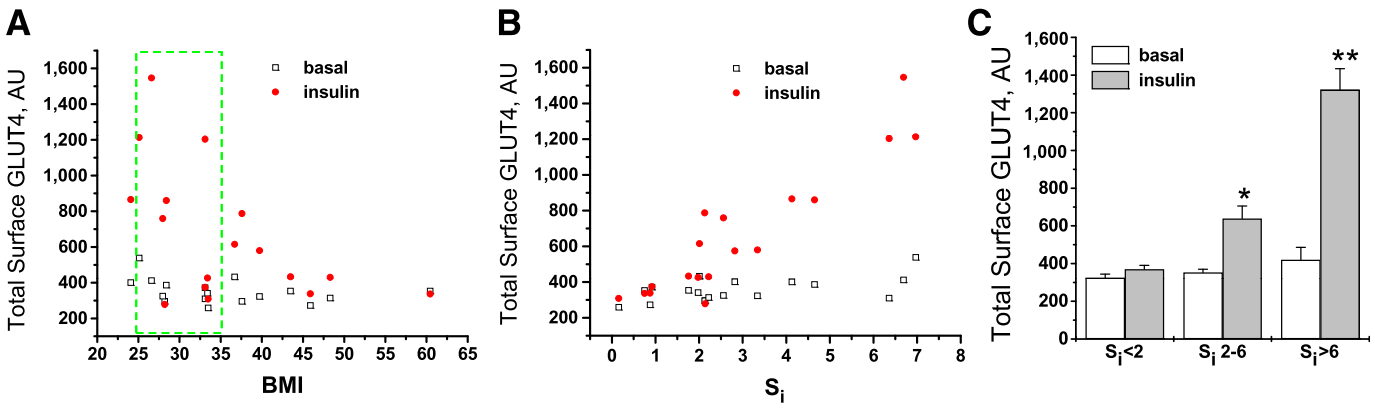

FIG. 4. Insulin-stimulated cell-surface GLUT4. Cell-surface GLUT4 was measured using an HA antibody-binding assay in transfected, isolated, nonpermeabilized human adipose cells. *A*: Total cell-surface GLUT4 measured in basal (black squares) and insulin-stimulated (red circles) cells, and plotted against BMI. Cells from subjects with BMI within the narrow range of 25–35 (dashed box) that displayed highly variable insulin responses were further analyzed for effects of S_i independent of BMI (Supplementary Fig. 3). *B*: Total surface GLUT4 measured in basal and insulin-stimulated cells, and plotted against S_i. *C*: GLUT4 distribution on the cell surface was further characterized by dividing the human subjects into groups, with impaired insulin sensitivity (S_i <2, n = 6), lowered insulin sensitivity (S_i 2–6, n = 9), and normal insulin sensitivity (S_i >6, n = 3). Mean ± SEM; *P < 0.05; **P < 0.01.

GSV, and the kinetics of GSV fusion to the cell surface were all independent of S_i.

Of interest, we found in adipose cells from subjects within a narrow BMI range of 25–35 GLUT4 trafficking parameters were only weakly dependent on BMI. Thus, our results demonstrate that S_i is a much better predictor than obesity of adipose-cell insulin responsiveness, despite the fact that the major portion of insulin-stimulated systemic glucose clearance occurs in muscle. Furthermore, in the current study, adipose cells in culture do preserve their insulin sensitivity despite the absence of humoral factors known to modulate insulin action on adipose tissue in vivo. Our data thus suggest that insulin-sensitive glucose transport is at least partly an inherent property of the isolated cells.

Results herein demonstrate that while the molecular machinery of translocation, tethering, and fusion of GSVs is intact in cultured adipose cells, even from the most insulin-resistant subjects, the extent to which tethering and fusion can be stimulated by insulin is dysfunctional in cells from resistant subjects. Because of the limitations of tissue availability, we could not evaluate the activation of insulin signaling pathways or validate glucose uptake on the same samples that we transfected and processed for TIRF microscopy. However, in the absence of evidence for the regulation of GLUT4 intrinsic activity (20), glucose transport is thought to correspond directly to the number of PM GLUT4, and thus our cell-surface GLUT4 data likely reflect actual glucose uptake. Future studies will be necessary to determine the possible roles of the signaling cascades in the cellular mechanisms of insulin resistance affecting GLUT4 vesicle tethering and fusion. Nevertheless, we have recently shown (24) a clear effect of insulin on GLUT4 cluster dynamics, which, in the current study, is maintained in the cells from the most insulin-resistant subjects (data not shown); this observation suggests that insulin signaling per se cannot fully account for the diminished insulin action on GLUT4 dynamics. GLUT4 exocytosis, vesicle-associated membrane protein 2, syntaxin-4, and its regulatory protein Munc18c are additional candidates for the ultimate regulatory mechanism of glucose transport (25). The current findings should also be evaluated in the context of specific cellular properties, such as adipose cell size, and compared among cells isolated from different fat depots.

ACKNOWLEDGMENTS

This work was supported by the Intramural Research Programs of the National Institute of Diabetes and Digestive and Kidney Diseases and the Eunice Kennedy Shriver National Institute of Child Health and Human Development, National Institutes of Health.

No potential conflicts of interest relevant to this article were reported.

V.A.L., J.Z., S.W.C., and K.G.S. initiated the concept of the study. V.A.L., J.-P.L., and K.G.S. performed all the experiments on cells and tissue isolated from biopsy samples. M.C.S. was in charge of the clinical protocol, recruitment of the subjects, and assessment of all the clinical parameters (e.g., BMI, S_i). All authors contributed to the interpretation of the data and writing of the manuscript. V.A.L. performed the statistical analyses. J.Z. is the guarantor of this work and, as such, had full access to all of the data in the study, and takes responsibility for the integrity of the data and the accuracy of the data analysis.

Parts of this study were presented in abstract form at the 73rd Scientific Sessions of the American Diabetes Association, Chicago, Illinois, 21–25 June 2013.

The authors thank Paul Blank, Program in Physical Biology, Eunice Kennedy Shriver National Institute of Child Health and Human Development; and Arthur Sherman, Laboratory of Biological Modeling, National Institute of Diabetes and Digestive and Kidney Diseases, National Institutes of Health, for help with statistics.

REFERENCES

1. Abbasi F, Brown BW Jr, Lamendola C, McLaughlin T, Reaven GM. Relationship between obesity, insulin resistance, and coronary heart disease risk. J Am Coll Cardiol 2002;40:937–943
2. Reaven GM. Banting lecture 1988. Role of insulin resistance in human disease. Diabetes 1988;37:1595–1607
3. Calori G, Lattuada G, Piemonti L, et al. Prevalence, metabolic features, and prognosis of metabolically healthy obese Italian individuals: the Cremona Study. Diabetes Care 2011;34:210–215
4. Blüher M. Are there still healthy obese patients? Curr Opin Endocrinol Diabetes Obes 2012;19:341–346
5. Yang Q, Graham TE, Mody N, et al. Serum retinol binding protein 4 contributes to insulin resistance in obesity and type 2 diabetes. Nature 2005;436:356–362

6. Friedman JM, Halaas JL. Leptin and the regulation of body weight in mammals. Nature 1998;395:763–770
7. Klebanov S, Astle CM, DeSimone O, Ablamunits V, Harrison DE. Adipose tissue transplantation protects ob/ob mice from obesity, normalizes insulin sensitivity and restores fertility. J Endocrinol 2005;186:203–211
8. Kandror K, Pilch PF. Identification and isolation of glycoproteins that translocate to the cell surface from GLUT4-enriched vesicles in an insulin-dependent fashion. J Biol Chem 1994;269:138–142
9. Lizunov VA, Matsumoto H, Zimmerberg J, Cushman SW, Frolov VA. Insulin stimulates the halting, tethering, and fusion of mobile GLUT4 vesicles in rat adipose cells. J Cell Biol 2005;169:481–489
10. Bai L, Wang Y, Fan J, et al. Dissecting multiple steps of GLUT4 trafficking and identifying the sites of insulin action. Cell Metab 2007;5:47–57
11. Danielsson A, Ost A, Nystrom FH, Strålfors P. Attenuation of insulin-stimulated insulin receptor substrate-1 serine 307 phosphorylation in insulin resistance of type 2 diabetes. J Biol Chem 2005;280:34389–34392
12. Carvalho E, Eliasson B, Wesslau C, Smith U. Impaired phosphorylation and insulin-stimulated translocation to the plasma membrane of protein kinase B/Akt in adipocytes from Type II diabetic subjects. Diabetologia 2000;43:1107–1115
13. Smith U, Axelsen M, Carvalho E, Eliasson B, Jansson PA, Wesslau C. Insulin signaling and action in fat cells: associations with insulin resistance and type 2 diabetes. Ann N Y Acad Sci 1999;892:119–126
14. Abel ED, Peroni O, Kim JK, et al. Adipose-selective targeting of the GLUT4 gene impairs insulin action in muscle and liver. Nature 2001;409:729–733
15. Garvey WT, Huecksteadt TP, Matthaei S, Olefsky JM. Role of glucose transporters in the cellular insulin resistance of type II non-insulin-dependent diabetes mellitus. J Clin Invest 1988;81:1528–1536
16. Franck N, Stenkula KG, Ost A, Lindström T, Strålfors P, Nystrom FH. Insulin-induced GLUT4 translocation to the plasma membrane is blunted in large compared with small primary fat cells isolated from the same individual. Diabetologia 2007;50:1716–1722
17. Maianu L, Keller SR, Garvey WT. Adipocytes exhibit abnormal subcellular distribution and translocation of vesicles containing glucose transporter 4 and insulin-regulated aminopeptidase in type 2 diabetes mellitus: implications regarding defects in vesicle trafficking. J Clin Endocrinol Metab 2001;86:5450–5456
18. Boston RC, Stefanovski D, Moate PJ, Sumner AE, Watanabe RM, Bergman RN. MINMOD Millennium: a computer program to calculate glucose effectiveness and insulin sensitivity from the frequently sampled intravenous glucose tolerance test. Diabetes Technol Ther 2003;5:1003–1015
19. Lizunov VA, Lisinski I, Stenkula K, Zimmerberg J, Cushman SW. Insulin regulates fusion of GLUT4 vesicles independent of Exo70-mediated tethering. J Biol Chem 2009;284:7914–7919
20. Holman GD, Kozka IJ, Clark AE, et al. Cell surface labeling of glucose transporter isoform GLUT4 by bis-mannose photolabel. Correlation with stimulation of glucose transport in rat adipose cells by insulin and phorbol ester. J Biol Chem 1990;265:18172–18179
21. Rodbell M. Metabolism of isolated fat cells. I. Effects of hormones on glucose metabolism and lipolysis. J Biol Chem 1964;239:375–380
22. Stenkula KG, Said L, Karlsson M, et al. Expression of a mutant IRS inhibits metabolic and mitogenic signalling of insulin in human adipocytes. Mol Cell Endocrinol 2004;221:1–8
23. Stenkula KG, Lizunov VA, Cushman SW, Zimmerberg J. Insulin controls the spatial distribution of GLUT4 on the cell surface through regulation of its postfusion dispersal. Cell Metab 2010;12:250–259
24. Lizunov VA, Stenkula K, Troy A, Cushman SW, Zimmerberg J. Insulin regulates Glut4 confinement in plasma membrane clusters in adipose cells. PLoS One 2013;8:e57559
25. Aran V, Bryant NJ, Gould GW. Tyrosine phosphorylation of Munc18c on residue 521 abrogates binding to Syntaxin 4. BMC Biochem 2011;12:19